Hindawi
Journal of Engineering
Volume 2022, Article ID 6214470, 13 pages
https://doi.org/10.1155/2022/6214470

Research Article

Performance Analysis of the Milk Pasteurization Process Using a Flat Plate Solar Collector

Surafel Tigabe,[1] Addisu Bekele ,[2] and Vivek Pandey [2]

[1]*Mechanical Engineering Department, University of Gondar, Gondar, Ethiopia*
[2]*Mechanical Engineering Department, Adama Science and Technology University, Adama, Ethiopia*

Correspondence should be addressed to Addisu Bekele; addisu2009@gmail.com

Received 26 April 2022; Revised 11 August 2022; Accepted 6 September 2022; Published 29 September 2022

Academic Editor: Natt Makul

A large share of Ethiopia's milk production comes from its rural areas. However, this milk does not undergo further processing into dairy products on a large scale due to lack of conventional energy sources such as electricity and gas. Hence, the country is not utilizing its milk resources to the maximum possible. In this study, the possible use of solar energy for the milk pasteurization process is investigated by using a flat plate solar collector (FPSC) with and without reflectors integrated. Reflectors added to the FPSC have augmented the incident solar radiation on the collector from 0.27–0.91 kW/m^2 to 0.36–1.18 kW/m^2. The thermal efficiency obtained for the FPSC with reflectors integrated is 51.8% whereas that of the collector without reflectors integrated is 46.2%. Likewise, the exergy efficiency is found to be 5.43% for the collector integrated with reflectors and 2.53% for the collector without reflectors. Also, an increase in the daily processed milk production of 18% is observed in September and 16% in November by using the solar collector with reflectors integrated. The quality of pasteurized milk is checked by using the methylene blue reduction test (MBRT) method, and it indicates a better quality of pasteurized milk when compared with raw milk. Therefore, this study shows that the use of solar energy for milk pasteurization has great potential to increase the shelf life of milk, and it can be used as an instrument to improve the quality of life of people living in rural areas.

1. Introduction

In Ethiopia, the traditional milk production system accounts for about 97-98% of the total annual milk production [1, 2]. From the estimated amount of collected milk, households consume 85%, while 8% of milk is processed in order to increase the product shelf life and 7% is sold [3]. This indicates that milk productivity and commercialization are low because of the small number of dairy processing units, traditional techniques of milk production in rural areas, and transportation difficulties from production areas to markets.

Due to the lack of infrastructure, milk is an important component of the rural economy, but only 7% is marketed out of the rural areas of production [4]. This is the great gap in the country, which results in a shortage in the supply of dairy products to urban areas. Another concern is related to the safety of dairy products concerning foodborne disease, especially in developing countries where the production of milk and various dairy products takes place under hygienically poor production systems [5].

The best-known heat treatment in a milk processing plant is pasteurization, which is carried out between 60 and 75°C. Pasteurization extends the shelf life of milk, improves milk quality, and minimizes the risk of milk poisoning [6]. Furthermore, Ethiopia is ranked as one of the top 20 countries with a lack of access to electricity. The majority of people in Ethiopia are living in rural areas, where modern energy services are unavailable [7]. Fortunately, Ethiopia is blessed with a large amount of solar radiation for a maximum number of hours, and this abundant resource can be used as the primary source of energy for heating procedures [8]. Recently, various solar thermal collector designs have been proposed, and these may be classified into two general types based on concentration ratio, namely, flat plate collectors and concentric collectors [9].

Table 1: Milk pasteurization standards [12].

Temperature (°C)	Holding time
63	30 min
72	15 s
89	10 s
90	0.5 s
94	0.1 s
96	0.05 s
100	1.1 s

Mihret et al. [10] reviewed the dairy sector in Ethiopia and identified the causes of its underdeveloped state such as low milk productivity, low milk quality, poor organization of development actions in the subsector and the chain, lack of market-oriented producers, and lack of infrastructures.

Broadly, pasteurization can be classified as low-temperature or high-temperature pasteurization methods either by the batch or continuous process. Low-temperature pasteurization aims at killing pathogenic microorganism and reducing spoilage. High-temperature pasteurization aims at killing vegetative pathogenic and spoilage bacteria [11]. During pasteurization, the rate of destruction of pathogens is dependent on both the temperature and time at which milk is held. Pasteurization temperature and holding time recommendations of the U.S. Public Health Service/ Food and Drug Administration as per the Standards of Pasteurized Milk Ordinance (PMO) are listed in Table 1.

Nielsen and Pedersen [13] designed a control system for solar-based milk pasteurization for villages in Tanzania. They have found that 71°C is the best temperature for pasteurization. The major problem in their system was the attainment of a constant temperature during startup and normal production conditions. Wayua et al. [14] designed and analyzed a flat plate solar milk pasteurizer for arid pastoral areas of Kenya. They could get an optimum quantity of milk after pasteurization at 69.1°C. Atia et al. [15] designed and analyzed a pasteurization system using a flat plate collector in remote areas and village communities who are deprived of the availability of electricity and gas. In their study, liquid milk was pasteurized by using a 1.2 m^2 flat plate solar collector. Franco et al. [16] fabricated a low-cost solar concentrator without sun-tracking mechanism for pasteurizing goat milk for cheese production. The system used a Fresnel-type concentrator with a focal distance of 20 cm to reduce sensitivity in sunlight tracking. This device had no automatic tracking system. Atia et al. [17] fabricated a solar milk pasteurization device with a dual-axis, closed-loop control, and sun-tracking device. The device operation was based on the contrast of sunlight levels using light-dependent resistors (LDRs) and an op-amp chip. Degefa [18] studied the performance analysis of a solar energy system for small-scale milk pasteurization with a coil heat exchanger fully immersed within a milk storage tank. Mallett [19] developed a low-cost parabolic solar reflector unit for the pasteurization of raw milk in rural areas of Southern Africa for those lacking adequate infrastructure, including electricity. The parabolic trough system was tested by heating water up to the necessary pasteurization temperatures. In each of the receiver tubes, solar absorber coatings were used, and temperatures above 75°C were achieved with all of them. The system was then tested using milk, and the same temperature ranges were obtained. This allowed milk to be successfully pasteurized.

The performances of most FPSC devices are based on energy analysis which essentially accounts only for energy entering and exiting the system. An additional analysis, which is called exergy analysis, can identify the cause, location, and magnitude of system inefficiencies and gives a better measure of performance in terms of quality of energy. Therefore, it is essential to consider both energy and exergy analysis for estimating the thermal performance and optimizing the working parameters of the FPSC [20].

The use of solar energy paired with pasteurization of milk may be a good alternative to solve the energy problem caused by the scarcity of fuel or electricity and to ensure a healthy milk supply. However, there is no experimental study conducted yet on the use of milk pasteurization using solar energy in Ethiopia. Likewise, improving the performance of the flat plate solar collector for milk pasteurization done by previous researchers using various techniques is very vital for implementing the technology in the rural areas of Ethiopia.

Hence, the aim of this study is to develop a prototype of a milk pasteurization system using a flat plate solar collector and analyze its performance in detail. This study will benefit the community by decreasing the wastage of milk production in rural areas, increasing the shelf life of milk, and increasing the marketing potential and hence improve the economy of the farmers.

2. Methodology

This study was conducted at Gondar, Ethiopia, located at 12.6° N latitude and 34.446° E longitude in the northern hemisphere with an elevation of 2133 meters above sea level. The climate is mild and generally warm temperate. The average maximum ambient temperature is 29.7°C and the average minimum ambient temperature is 14.3°C.

In this study, both theoretical and experimental approaches are used. The theoretical approach applies governing equations for the analysis of each component to study the overall system performance of milk pasteurization by using FPSC. The prototype of the collector is developed after completing the sizing and selection of materials for each component. For designing the FPSC, the solar potential of Gondar is predicated based on the sunshine hours data collected from the Ethiopian Meteorological Agency (EMA). Finally, the theoretical and numerical formulations leading to the energy and exergy efficiencies of the collector are analyzed.

Several methods relate the global radiation to climatic conditions such as sunshine hours, temperature, humidity, cloudiness, and precipitation [21]. Among these, sunshine hour is the most widely and commonly used parameter for study. The first empirical method for estimating global radiation based on sunshine duration is the model presented by Prescott [22]. They calculated the monthly average global radiation based on extraterrestrial radiation on a horizontal surface. Figure 1 shows the values of five-year average

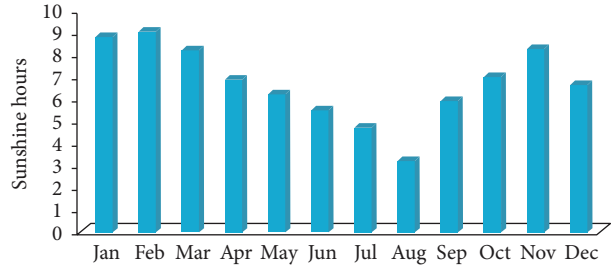

Figure 1: Monthly variation of sunshine hours.

sunshine hours (2015–2019), accessed from the Ethiopian Meteorological Agency (EMA).

The detail specifications of the FPSC used in the experimental setup are summarized in Table 2.

2.1. Energy Analysis of the Flat Plate Solar Collector. The performance of a solar collector is identified using energy balance that indicates the distribution of incident solar energy into useful energy gain, thermal loss, and optical loss. An essential notation for energy analysis of any thermal system is only related to conservation of energy, which can be evaluated through energy balance calculation under steady state condition.

The useful energy gain in terms of the fluid inlet and outlet temperature is determined using the following expression:

$$Q_u = \dot{m}c_p(T_o - T_i). \tag{1}$$

The useful heat gain by the working fluid from the collector (Q_{uc}) can also be analyzed in terms of the fluid inlet temperature (T_{in}) as

$$Q_{uc} = A_c F_R(S - U_l(T_{\text{in}} - T_a)), \tag{2}$$

where F_R represents the collector heat removal factor, $S = (\tau\alpha I_T)$ represents the absorbed solar radiation per unit time, τ represents the transmissivity of the glass cover, α represents the absorptivity of the absorber plate, and I_T represents the incident solar energy per unit area.

The heat removal factor is the ratio of useful energy gained by the collector to the energy gained by the collector where it is entirely at the fluid inlet temperature. Determining the heat removal factor for a serpentine collector is more difficult than for a conventional header-riser flat plate collector because they have different performance in the internal heat transfer coefficient. Unlike the analysis of header-riser tube configuration of a flat plate collector where the fins between the tubes are assumed adiabatic at the center of the tube spacing, there is heat transfer between the tubes for a serpentine collector.

There are many formulations and equations developed and modified for serpentine flows, and the last modified equation is used for heat removal factor calculations with serpentines of arbitrary geometry, and the number of bends is given by [23]

Table 2: Specifications of FPSC.

Specifications	Value
Gross area	1.19 m^2
Area of the collector	1.18 m^2
Length of the tube	11 m
Outer diameter of the tube	12 mm
Thickness of the tube	0.5 mm
Length of the absorber plate	1.28 m
Width of absorber plate	0.92 m
Thickness of the glass	4 mm
Insulation thickness	5 mm
Air gap between the plate and glass	30 mm

$$F_R = \frac{\dot{m}C_p}{A_c U_l}\left[1 - \exp\left(\frac{A_c U_l F_1 (F_2 - 1)}{\dot{m}C_p}\right)\right], \tag{3}$$

where F_1 and F_2 are the parameters for determining collector heat removal factor which is a function of physical design parameters [23]:

$$\begin{aligned} F_1 &= \frac{N\kappa L}{U_l A_c}\,\frac{\kappa R(1+\gamma)^2 - 1 - \gamma - \kappa R}{[\kappa R(1+\gamma) - 1]^2 - (\kappa R)^2}, \\ F_2 &= \frac{1}{\kappa R(1+\gamma)^2 - 1 - \gamma - \kappa R}, \\ \kappa &= \frac{K\delta m}{(W - D_i)\sinh m}, \\ \gamma &= -2\cosh m - \frac{DU_l}{\kappa}, \\ m &= (W - D)\sqrt{\frac{U_l}{K\delta}}, \\ m &= (W - D)\sqrt{\frac{U_l}{K\delta}}, \end{aligned} \tag{4}$$

where D_i represents the tube inner diameter, and δ represents the plate thickness.

The thermal efficiency (η_{th}) of the solar collector is the ratio of the output useful energy to the absorbed solar energy, and it is expressed as

$$\eta_{\text{th}} = \frac{Q_u}{A_c(\tau\alpha)I_T}. \tag{5}$$

The overall heat lost coefficient from the collector is the sum of the heat lost from the top, the bottom, and the side heat losses, and it is expressed as follows:

$$U_l = U_t + U_b + U_s, \tag{6}$$

where U_t, U_b and U_s are the heat lost coefficients from the top, bottom, and side, respectively.

The top loss coefficient is expressed empirically as the following equation:

$$U_t = U_{\text{pg}} + U_{\text{ga}}. \tag{7}$$

The heat transfer coefficient from the absorber plate to the glass cover (U_{pg}) includes the thermal energy loss by convection and radiation.

The convective heat transfer coefficient (h_{1c}) of the top heat loss from the collector plate to the cover which is tilted at some angles is related to three dimensionless parameters, Nusselt number, N_u, the Rayleigh number, R_a, and the Prandtl number, P_r, expressed as follows:

$$h_{1c} = Nu\frac{K}{L},$$

$$N_u = 1 + 1.44\left[1 - \frac{1708}{R_a\cos(\beta)}\right]^{+}\left[1 - \frac{1708\sin(1.8\beta)^{1.6}}{R_a\cos(\beta)}\right] + \left(\frac{R_a\cos(\beta)^{1/3}}{5830}\right)^{+}, \tag{8}$$

where "+" exponent means only positive value in square bracket is considered and zero is to be used for negative value.

The Rayleigh number is expressed as

$$R_a = \frac{g\beta'\Delta T L^3 P_r}{v^2}. \tag{9}$$

The volumetric expansion coefficient β' is given by

$$\frac{1}{\beta'} = \frac{T_p + T_g}{2}, \tag{10}$$

where K represents the is plate thermal conductivity, g represents the gravitational constant, L represents the length between plate and glass, ΔT is the temperature difference between absorber plate and the glass cover, and v represents the kinematic viscosity of air.

The radiation heat transfer coefficient (h_{1r}) from the absorber plate to the glass cover is given by

$$h_{1r} = \varepsilon_{\text{eff}}\sigma\left(\frac{\left(T_p + 273\right)^4 - \left(T_g + 273\right)^4}{\left(T_p - T_g\right)}\right). \tag{11}$$

The effective emissivity (ε_{eff}) of the plate-glazing system is given by

$$\varepsilon_{\text{eff}} = \left[\frac{1}{\varepsilon_p} + \frac{1}{\varepsilon_g} - 1\right]^{-1}. \tag{12}$$

Hence, the total heat transfer coefficient from the absorber plate to the glass cover (U_{pg}) is simplified as

$$U_{\text{pg}} = Nu\frac{K}{L} + \varepsilon_{\text{eff}}\sigma\left(\frac{\left(T_p + 273\right)^4 - \left(T_g + 273\right)^4}{\left(T_p - T_g\right)}\right). \tag{13}$$

The heat transfer coefficient from the glass cover to the ambient (U_{ga}) includes the thermal energy loss by convection and radiation.

The convective heat transfer coefficient (h_{2c}) from the glass cover to the ambient is calculated by

$$h_{2c} = 2.8 + 3V_w, \tag{14}$$

where V_w is the wind speed.

The radiation heat transfer coefficient (h_{2r}) from the glass cover to the ambient is calculated from the following equation:

$$h_{2r} = \varepsilon_g\sigma\left(\frac{\left(T_g + 273\right)^4 - \left(T_{\text{sky}} + 273\right)^4}{\left(T_g - T_a\right)}\right). \tag{15}$$

The effective temperature of the sky (T_{sky}) is given as

$$T_{\text{sky}} = T_a - 6. \tag{16}$$

Hence, the total heat transfer coefficient from the glass cover to ambient (U_{ga}) is simplified as

$$U_{\text{ga}} = \left(2.8 + 3V_w\right) + \varepsilon_g\sigma\left(\frac{\left(T_g + 273\right)^4 - \left(T_{\text{sky}} + 273\right)^4}{\left(T_g - T_a\right)}\right). \tag{17}$$

The bottom loss coefficient (U_b) from the absorber plate to the ambient in the downward direction is by conduction through the insulation and convection through the bottom of the collector. It is assumed that the flow of heat is one dimensional and steady state condition, and the thickness of insulation provided that the thermal resistance associated with conduction dominates.

Therefore, by neglecting convective resistance at the bottom surface, the bottom loss coefficient can be expressed as

$$U_b = \frac{K_i}{\delta_b}, \tag{18}$$

where K_i represents the thermal conductivity of insulation, and δ_b represents the back insulation thickness.

The heat loss coefficient (U_s) at the side of the collector is expressed as

$$U_s = \frac{K_i}{\delta_e}\frac{A_s}{A_c}, \tag{19}$$

where δ_e represents the edge insulation thickness, A_s-$p^* d_e$, P represents the perimeter of the absorber plate, and d_e represents the height of the edge.

2.2. Exergy Analysis of the Flat Plate Solar Collector.

Exergy is defined as the maximum output of work that can be achieved relative to the environment, which is based on the second law of thermodynamics. The exergy analysis to the flat plate collector helps to achieve an optimum design and gives the direction to decrease exergy loss.

Considering a flat plate collector exergy analysis is performed based on the general form of exergy equation which is expressed as follows:

$$E_{x_{\text{in}}} - E_{x_{\text{out}}} = E_{x_d} + E_{x_l}, \tag{21}$$

where $E_{x_{\text{in}}}, E_{x_{\text{out}}}, E_{x_l}$, and E_{x_d} are the inlet, outlet, leakage (loss), and the destroyed exergy rates, respectively.

The inlet exergy rate $(E_{x_{\text{inf}}})$ due to the fluid flow can be calculated by

$$E_{x_{\text{inf}}} = \dot{m}C_p\left(T_i - T_a - T_a \ln\left(\frac{T_i}{T_a}\right)\right). \tag{22}$$

The inlet exergy due to radiation $(E_{x_{\text{inr}}})$ can be calculated by

$$E_{x_{\text{inr}}} = I_T A\left(1 - \frac{T_a}{T_s}\right), \tag{23}$$

where (T_s) is the surface temperature of sun which is equal to 5777 K.

Therefore, the total inlet exergy rate of the solar collector can be calculated as follows:

$$E_{x_{\text{in}}} = E_{x_{\text{inf}}} + E_{x_{\text{inr}}}. \tag{24}$$

The outlet exergy accounts for the exergy rate of outlet fluid which can be calculated as follows:

$$E_{x_{\text{out}\,f}} = -mC_p\left\{(T_o - T_a) - T_a \ln\left(\frac{T_o}{T_a}\right)\right\}. \tag{25}$$

The destructed exergy compromises of three terms. The first term is caused due to the heat leakage from absorber plate to the ambient, and it is calculated as

$$E_{d_{\text{leak}}} = A_p U_{\text{ga}}\left(T_p - T_a\right)\left[1 - \frac{T_a}{T_p}\right]. \tag{26}$$

The second part is caused by the temperature difference between the absorber plate and the sun which is calculated by

$$E_{d_{p-s}} = I_T A_c \eta_0\left(\frac{T_a}{T_p} - \frac{T_a}{T_s}\right), \tag{27}$$

where T_s is the apparent sun temperature as exergy source which is assumed to be 5700 K.

The third part is caused by the temperature difference between the absorber plate and the working fluid, which is calculated by

$$E_{d_{p-f}} = mC_p T_a\left\{\left(\ln\frac{T_0}{T_i}\right)\left(\frac{T_0 - T_i}{T_p}\right)\right\}. \tag{28}$$

Therefore, the total distracted energy is calculated by

$$E_d = E_{d_{p-s}} + E_{d_{p-f}} + E_{d_{\text{leak}}}. \tag{29}$$

The exergy efficiency is the ratio of the increase in working fluid flow exergy to the inlet exergy by solar radiation. Hence, the exergy efficiency can be evaluated as

$$\eta_{\text{ex}} = \frac{E_{x_{\text{outf}}} - E_{x_{\text{inf}}}}{E_{x_{\text{inr}}}}. \tag{30}$$

3. Experimental Setup

The experimental setup was constructed and tested at Gondar city of Ethiopia (12.6°N latitude and 34.446°E longitude). All the experiments are performed during the months of September and November, between 8 a.m and 4 p.m. The FPSC consists of a single glass cover, absorber plate, insulation, serpentine shaped copper tube, controlling valve, and fresh milk tank. It is mounted on a wooden frame built to support the collector at the optimum tilt angle (β) of 27.6°. The photographs of the experimental setup including FPSC without and with reflectors integrated and schematic diagram are shown in Figures 2(a), 2(b), and 2(c), respectively.

A digital thermometer with a range of −55°C to + 148°C (Figure 3(a)) is used to measure the ambient temperature, absorber plate temperature, glass temperature, and the inlet and outlet milk temperatures. For controlling the outlet temperature of milk, a 12 V relay dual LED digital thermostat temperature controller is installed in the outlet pipe near to the outlet controlling valve as shown in Figure 3(b), and the flow of milk outlet is controlled by an opening valve.

4. Experimental Procedure

The flat plate solar collector was designed for milk pasteurization at a constant milk flow rate of 0.01 kg/s. The first experiment was conducted to study the performance of solar thermal collectors with and without reflectors by assuming that heat transfer and fluid flow rate are in steady state conditions. The second experiment is performed to ascertain the production rate of pasteurized milk by retaining the milk flow in the collector for the recommended pasteurization time at a given temperature.

The quantity of pasteurized milk for given a pasteurization time and temperature can be calculated by

$$q_b = V^* t, \tag{31}$$

where q_b is the quantity of milk per batch, and V is the volume flow rate of milk.

The daily quantity of pasteurized milk per day (q_{day}) can be calculated by

$$q_{\text{day}} = \sum_{i=1}^{n} q_b(i). \tag{32}$$

4.1. Microbiological Quality Test of Raw and Pasteurized Milk. In order to determine the microbiological quality of raw and pasteurized milk, there are several tests commonly used,

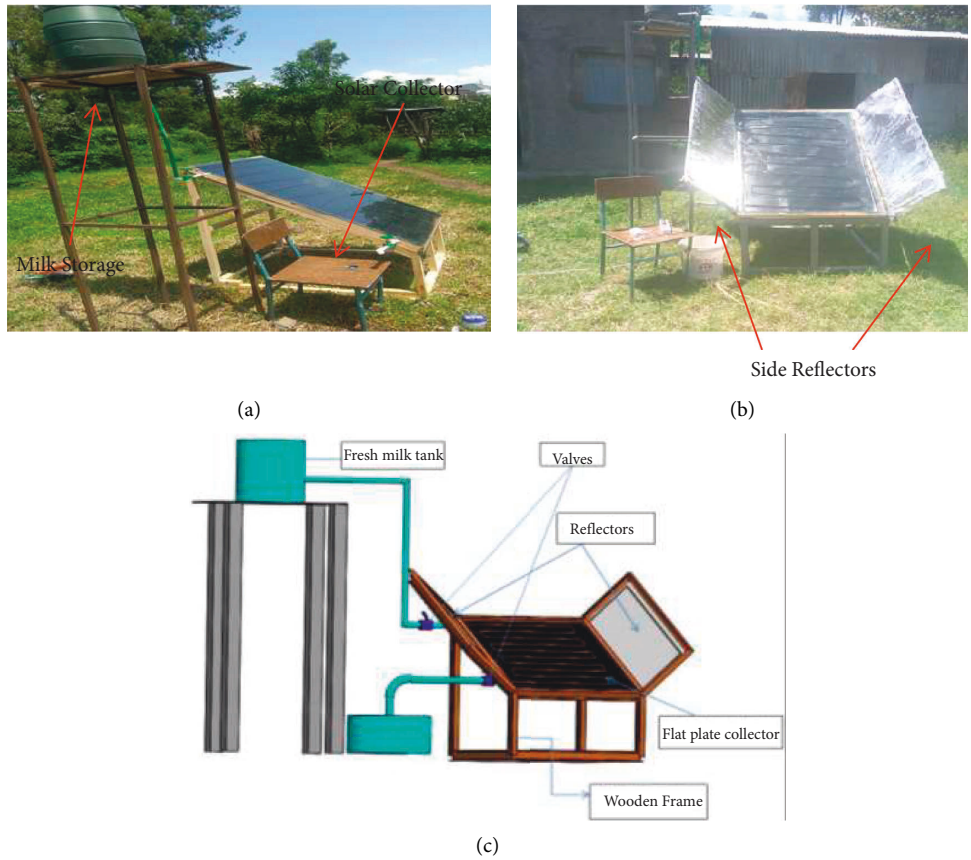

Figure 2: Experimental setup: (a) FPSC without reflector, (b) FPSC with reflector integrated, and (c) schematic of FPSC with reflector integrated.

including the standard plate count (SPC), psychotropic bacteria count (PBC), coliform count (CC), somatic cell count (SCC), and methylene blue reduction test (MBRT) [24]. Among these, MBRT was selected to assess the microbiological quality of pasteurized and raw milk due to its rapid, simple, and inexpensive methodology. The main principle of MBRT is to determine the quality of milk based on observing the change in color of milk by adding methylene blue. The color disappears more or less quickly [25]. Methylene blue is a blue colored redox indicator dye, and it loses its color when in contact with oxygen and harmful substances from microbial metabolism within milk [26]. The rate of reduction of methylene blue is, therefore, directly related to the bacterial load in milk. The grading of milk as per MBRT is given in Table 3 [27].

For the quantitative MBRT, 10 mL of raw milk sample is incubated at 37°C in a waterbath with 0.5 mL of methylene blue, as shown in Figure 4. The time (in hours) for the blue coloration to disappear is measured according to the technique described in ISO 4833-2:2013 [28].

5. Results and Discussion

The ambient air temperature, inlet temperature, and outlet temperature of milk are recorded from 8:00 hr to 16:00 hr. The estimated hourly variation of global, beam and diffuse radiation, and radiation falling on the surface of the collector with and without reflectors, which is tilted at an angle of 27.6° during the months of September and November, is shown in Figure 5.

5.1. Hourly Variation of Measured Temperature Difference. The hourly variations of the inlet temperature of milk, outlet temperature of milk, and ambient temperature for a collector without and with reflectors are shown in Figures 6 and 7, respectively. It is observed that the outlet temperature of milk increases in proportion to the incident solar radiation intensity. The maximum outlet temperature for a collector without reflectors is 44.9°C and 49.4°C in September and November, respectively. Similarly, the maximum outlet temperature for a collector with a reflector is 49.2°C and 52.2°C in September and November, respectively. This shows that the outlet temperature of milk increases with an increase in solar radiation. Therefore, addition of the reflectors to the solar collectors aids in increasing the solar intensity and, thereby, the outlet temperature of the milk.

5.2. Hourly Useful Heat Gain. The temporal variations of useful heat gain of the solar collector with and without reflectors integrated are shown in Figure 8. The useful heat gain of the collector increases in proportion to the solar radiation intensity. The maximum useful heat gain obtained

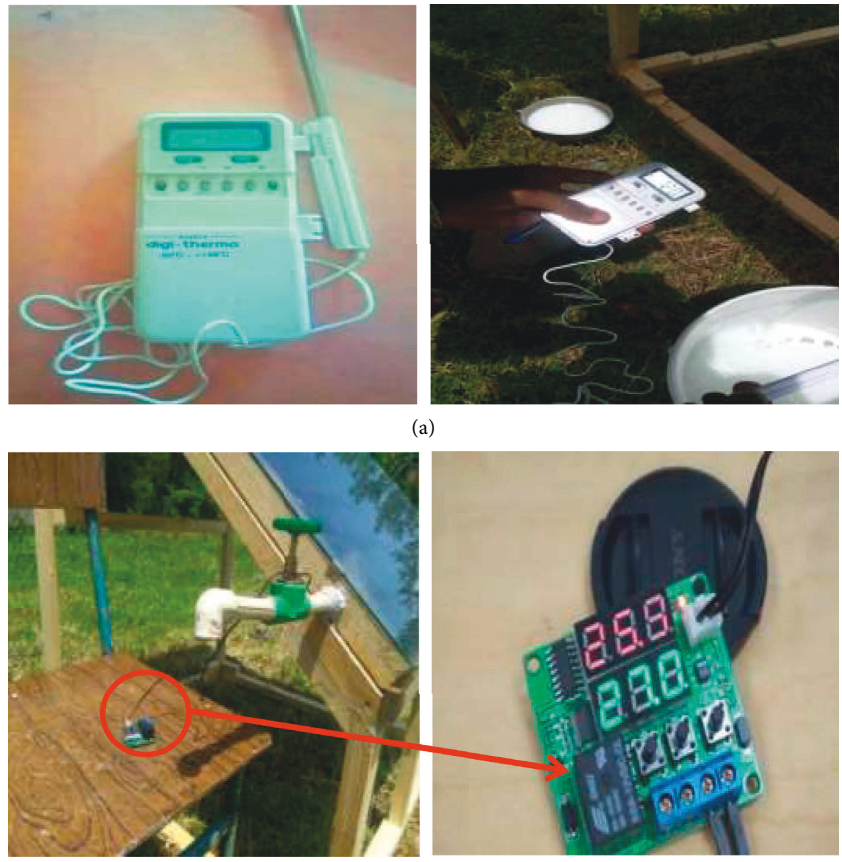

Figure 3: (a) Digital thermometer. (b) 12 V relay dual LED digital thermostat temperature controller.

Table 3: Grading of milk on the basis of MBRT.

Quality of milk	Decolourization time
Excellent	More than 8 hours
Good	Between 6 and 8 hours
Fair	Between 2 and 6 hours
Poor	Less than 2 hours

from FPSC integrated with reflectors is 750.63 W in September and 809.14 W in November. The minimum useful heat gain obtained from FPSC without reflectors integrated is 581.64 W in September and 679.89 W in November. Therefore, the useful heat gain achieved by FPSC with reflectors integrated is 29% higher for the month of September and 19% higher for the month of November when compared with that of FPSC without reflectors integrated.

5.3. Collector Heat Loss Coefficient. Figure 9 shows the effects of the difference in collector plate temperature and ambient temperature on the collector heat loss coefficient. It is observed that the overall heat loss coefficient increases when the inlet temperature increases and also as the temperature gradient between the absorber plate and the ambient increases. The heat loss coefficient of the collector varies from 6.68 to 6.94 W/km^2 when the temperature difference is 15–55°C. The average heat loss coefficient of the collector is 6.85 W/km^2 and 6.91 W/km^2 for FPSC integrated with and without reflectors, respectively.

5.4. Thermal Efficiency of the Collector. Figure 10 shows the hourly variation of the thermal efficiency of the FPSC integrated with and without reflectors. The thermal efficiency is directly proportional to the outlet temperature of milk. The results show that the outlet temperature of milk starts increasing from 08:00 hr and attains maximum at 13:00 hr. Therefore, the maximum thermal efficiency occurs at around noon when the outlet temperature and solar radiation are at their peak. The maximum thermal efficiency is 51.8% for FPSC integrated with reflectors and 46.2% for FPSC without reflectors in November. These results show that integrating reflectors into FPSC increases the thermal efficiency of the collector by 5%. Atia et al. [22] reported similar results for pasteurization of milk using a FPSC.

5.5. Exergy Analysis. In order to make a detailed analysis of the exergetic efficiency of the collector, the leakage exergy and destructed exergy owing to the collector components are taken into consideration. As shown in Figures 11 and 12 with an increase in the ambient temperature, the exergy also increases. All maximum values were found to occur in

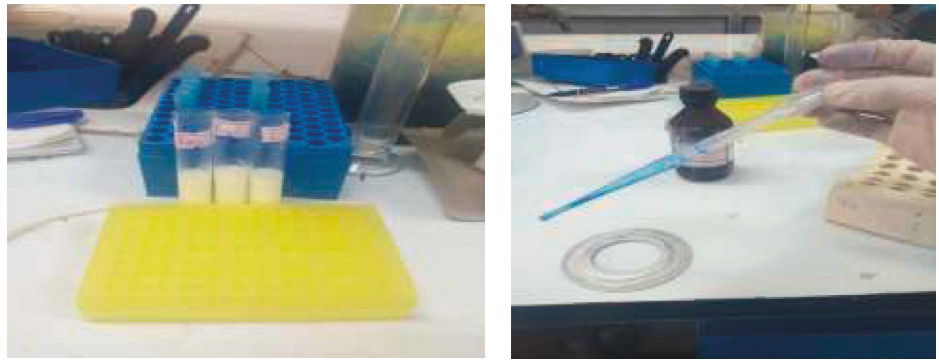

(a) (b)

Figure 4: (a) Milk samples (raw milk, heat-treated milk, and pasteurized milk). (b) Materials and equipment used for MBRT.

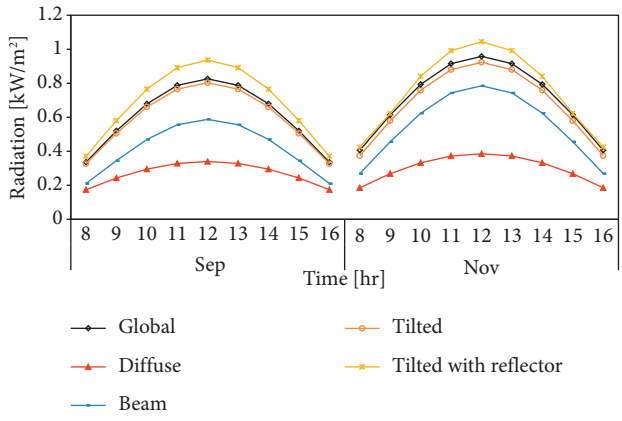

Figure 5: Estimated hourly variation of global solar radiation in Gondar on the month of September and November.

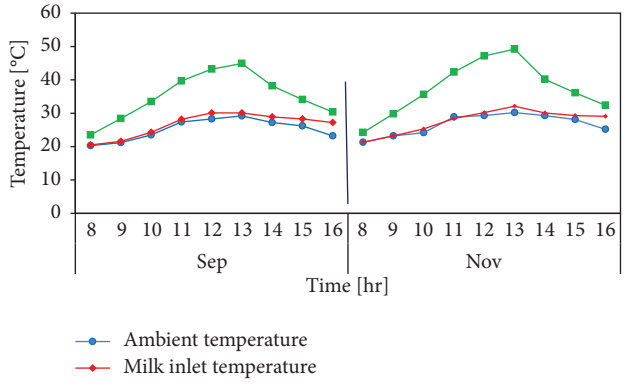

Figure 6: Hourly variation of ambient temperature, milk inlet temperature, and milk outlet temperature for a collector without reflector.

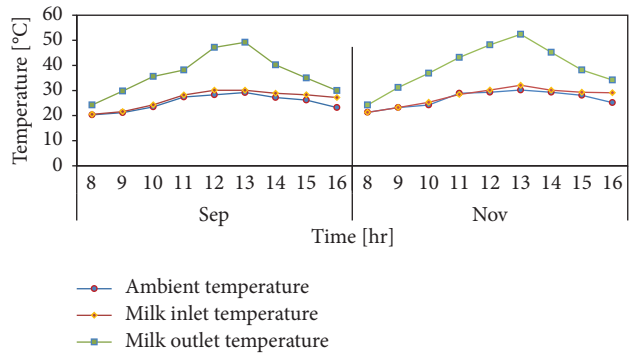

Figure 7: Hourly variation of ambient temperature, milk inlet temperature, and milk outlet temperature for a collector with reflector.

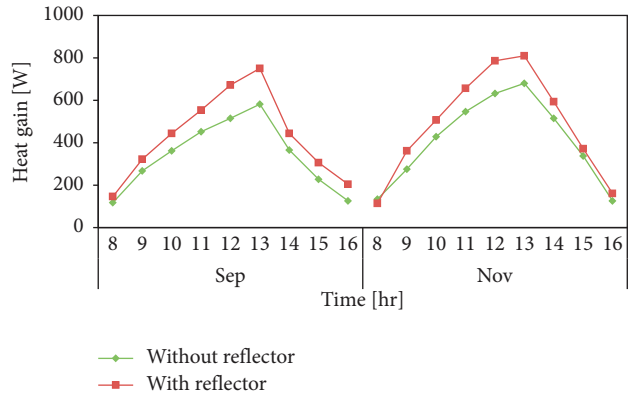

Figure 8: Variation of useful heat gain of the collector with time.

November. In September, the inlet exergy of the working fluid and absorbed solar radiation are in the range of 1023–386 W and 458–1094 W for the FPSC integrated with and without reflectors, respectively. The outlet exergy of the working fluid is between 3.52–22.8 W and 2.94–18.25 W for the FPSC integrated with and without reflectors, respectively. The destructed exergy is between 272–777.14 W and 245.64–914.2 W for the FPSC integrated with and without the reflectors, respectively. All maximum exergy values occur at midday when the solar radiation value is at its peak. In November, the inlet exergy of the working fluid and absorbed solar radiation is in the range 1154–431 W and 1023–409.21 W for the FPSC integrated with and without reflectors, respectively. The outlet exergy value is between 4.32–20.4 W and 5.36–26.8 W for the FPSC integrated with and without reflectors. The destructed exergy is between 283.14–784.14 W and

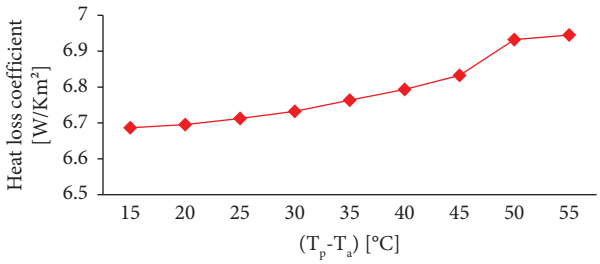

Figure 9: Effects of the temperature difference between the absorber plate and ambient on the overall heat loss coefficient of the collector.

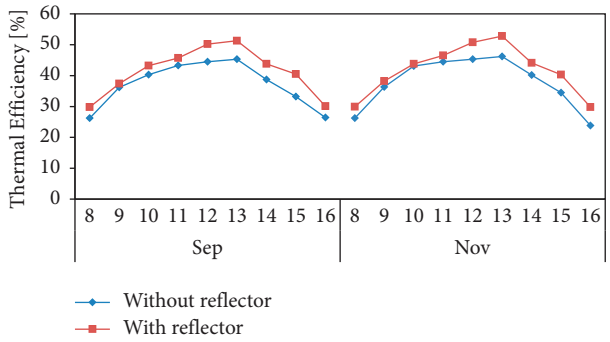

Figure 10: Hourly variation of thermal efficiency with and without reflectors.

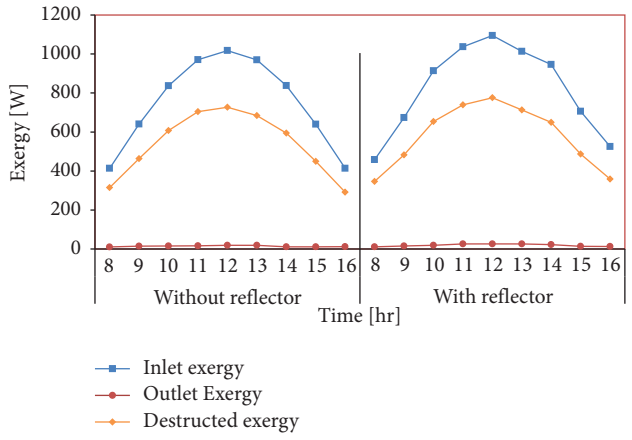

Figure 11: Exergy of the collector without and with reflector based on time of the day in September.

256.64–916.2 W for the FPSC integrated with and without reflectors, respectively.

5.6. Comparison of Destructed Exergy Rate with and without Reflectors. The destructed exergy rate due to heat transfer from the absorber plate to the environment increases with an increase in the ambient and plate temperatures. As shown in Figure 13, as the ambient temperature increases, the exergy leakage increases, but the increment in ambient temperature is

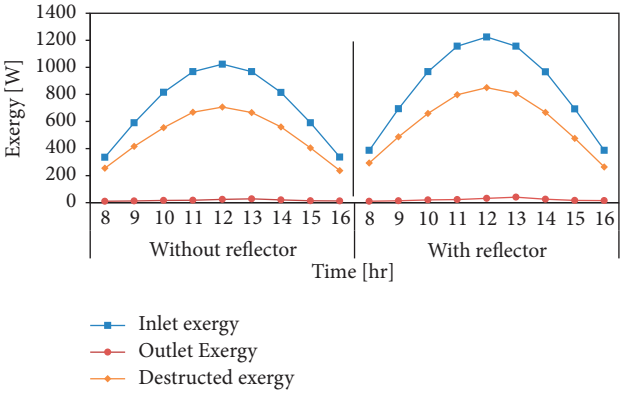

Figure 12: Exergy of the collector without and with reflector based on time of the day in November.

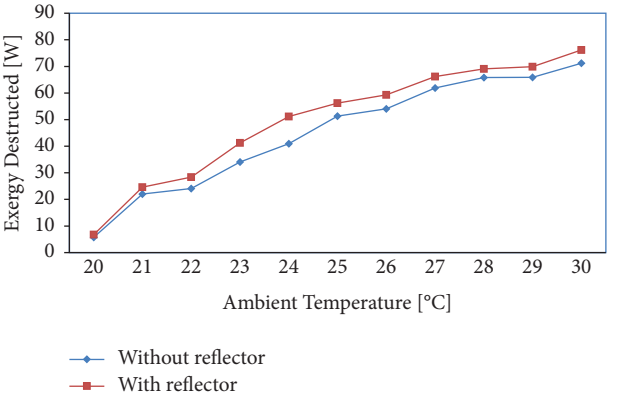

Figure 13: Variation of exergy loss related to ambient temperature for FPSC integrated with and without reflectors.

very slow compared to the plate temperature. Therefore, with equivalent ambient temperature variation, the collector integrated with reflectors has a high leakage exergy rate compared to the collector without reflectors. This is due to high plate temperature of the collector when integrated with reflectors.

The exergy loss rate due to the temperature difference between solar radiation and absorber plate increases with the increment of ambient temperature and incident solar radiation. The increasing tendency of absorber plate temperature has a great effect on exergy destruction. As shown in Figure 14, the value of destructed exergy due to the temperature difference between solar radiation and absorber plate is small in the collector integrated with reflectors compared to the collector without reflectors. Therefore, as shown in Figure 14, the largest exergy loss is caused by the temperature difference between the absorber plate and the sun, which is about 89.21% and 89.08% of the total inlet exergy rate for FPSC integrated with and without reflectors, respectively.

It is observed from the result that the increasing absorber plate temperature effect is higher on the collector integrated with reflectors. This shows that the destructed exergy is more affected by solar radiation when the ambient temperature is constant as shown in Figure 15.

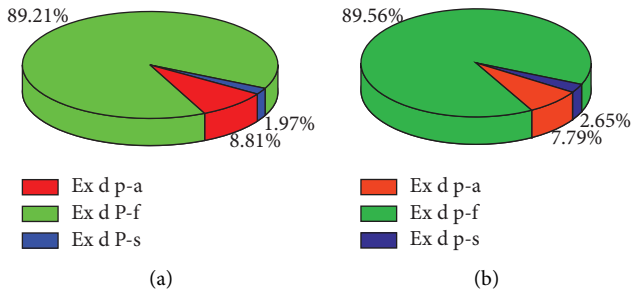

Figure 14: Comparison of exergy destruction (a) with and (b) without reflectors.

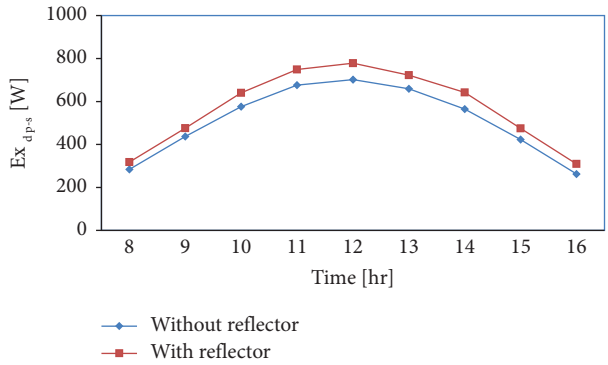

Figure 15: Variation of destructed exergy caused by temperature difference between sun and absorber plate versus time.

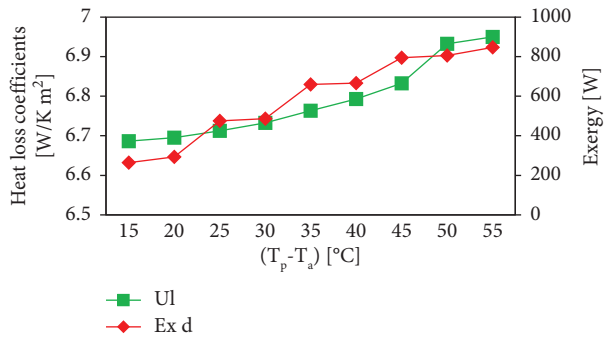

Figure 16: Effects of the temperature difference between the absorber plate and environment on overall heat loss coefficients and exergy destructions for the collector.

The overall heat loss coefficient and exergy destruction increase as the temperature difference between the collector plate and ambient temperature increases as shown in Figure 16.

5.7. Exergetic Efficiency. Figure 17 shows the variation of exergy efficiency versus time. The results indicate that the exergy efficiency of the collector without reflectors starts increasing from 0.17% at 08:00 hr and reaches a maximum value of 2.53% at 12:00 hr, and thereafter, it starts decreasing

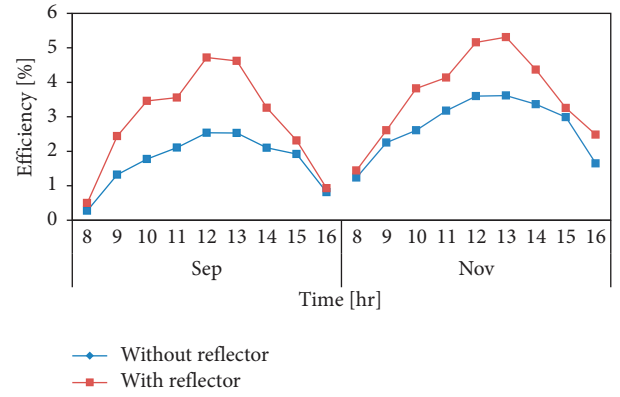

Figure 17: The variation of exergy efficiency versus time.

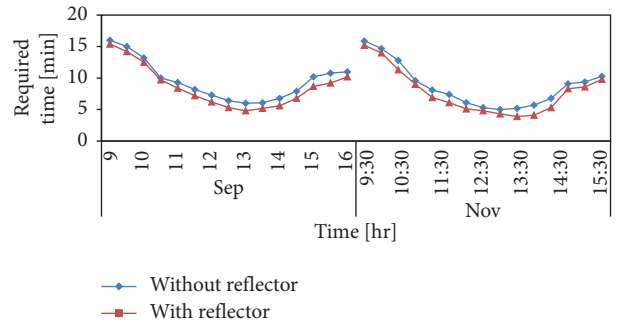

Figure 18: Time to attain pasteurization temperature.

as the solar radiation decreases. Additionally, the exergy efficiency of the collector starts increasing from 0.49% and reaches a maximum value of 4.71% in September. Similarly, in November, the exergy efficiency reaches a maximum of 5.43%, starting from 0.52%. This shows that with an increase in solar radiation, there is an increase in the heat gain and exergy efficiency.

5.8. Time to Attain Pasteurization Temperature. Figure 18 shows the time to reach pasteurization temperature (72°C) between 09:00 hr and 16:00 hr. The result shows that the collector with a reflector needs a shorter time to attain pasteurization temperature compared to the collector without reflectors. The minimum time to attain pasteurization temperature is at noon in September, which is 4.2 min and 6 min for FPSC integrated with and without reflectors, respectively. Also, in November, it is 3.9 min and 5.72 min for FPSC integrated with and without reflectors, respectively.

5.9. Quantity of Solar-Pasteurized Milk. Figure 19 shows the quantity of pasteurized milk with respect to time of day. The maximum quantity of pasteurized milk per day is achieved at noon due to peak solar radiation at noon. The daily pasteurized milk in September is 69.19 l/day and 58.59 l/day, and in November, it is 70.2 l/day and 60.24 l/day for FPSC integrated with and without the reflectors, respectively.

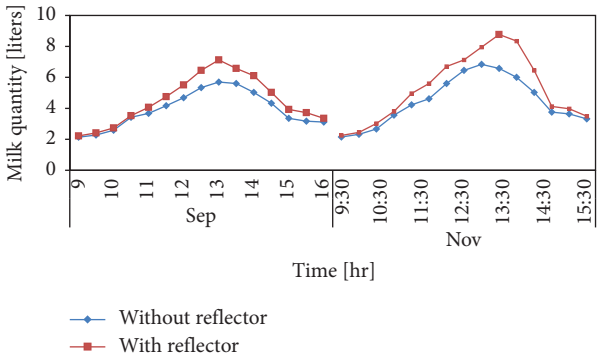

Figure 19: The quantity of pasteurized milk with respect to the time of the day.

Table 4: Comparison of thermal efficiency and quantity of pasteurized milk (liter per day) with the present study with literature for FPSC without reflectors.

Parameter	Present study	Atia et al. [22]
Maximum η_{th}	46.2%	43%
Quantity of pasteurization per day	60.24 l/day	55.6 l/day

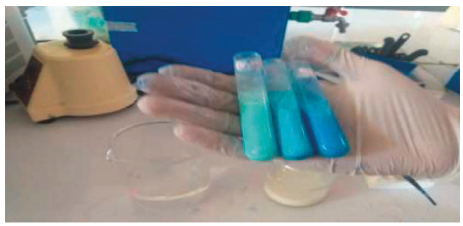

Figure 20: Result of MBRT after 30 min.

Therefore, by adding the reflectors to the collector, the quantity of pasteurized milk increases by 9 l/day.

As shown in Table 4, due to the addition of reflectors on both sides of the collectors, the thermal efficiency and the quantity of pasteurized milk is higher by 6.9% and 9%, respectively, compared to the results of Atia et al. [17].

5.10. Detection of Raw Milk, Heat-Treated Milk, and Pasteurized Milk Using the Methylene Blue Reduction Test (MBRT). The quality of milk is tested using MBRT, and the time required for methylene blue to become colorless is termed as methylene blue reduction time, which is an indicator of the milk quality. A smaller value of methylene blue reduction time implies a lower quality of milk and vice versa. Figure 20 shows that the raw milk starts changing its color after 30 min from the base time, and this indicates the quality of raw milk is very poor. The grading of milk samples with reduction time on the basis of MBRT is shown in Table 5.

The result shows that the methylene blue reduction time for raw milk is 1.10 h, which means that the quality is poor. However, after heating milk at pasteurization temperature, the methylene blue reduction time is increased to 4.30 h and the quality of milk is fair. Finally, the pasteurized milk (after heat treating milk and storing it in a refrigerator at 4°C) shows good quality due to destruction of contaminating microorganisms.

Table 5: Decolorization time and grading of milk samples.

Milk samples	Decolorization time (h)	Quality of milk
Raw milk	1.10	Poor
Heat-treated milk	4.30	Fair
Pasteurized milk	6.25	Good

6. Conclusions

In this study, a small-scale flat plate solar collector is designed, manufactured from locally available materials and tested for pasteurization of milk. The system performance is evaluated by using a flat plate solar collector with and without reflectors. By adding the reflectors on the collector, the incident solar radiation is found to increase from 0.27–0.91 kW/m^2 to 0.36–1.18 kW/m^2.

The experimental investigation onto the performance of flat plate solar collectors integrated with and without reflectors using energy and exergy analysis was carried out at a constant milk flow rate of 0.01 kg/s and the following results are highlighted:

(i) Thermal efficiency is directly proportional to the outlet temperature of milk, and the maximum efficiency obtained is 51.8% for FPSC integrated with the reflector and 46.2% without a reflector in November, adding a reflector onto the collector results in an efficiency increment of 5%.

(ii) The experimental results show that the maximum exergy efficiency of the flat plate solar collector without reflector is 2.53% and with reflector is 5.43% in November

The ability of the FPSC to pasteurize milk is tested experimentally with and without the reflector integrated. The results may be summarized as follows:

(i) The minimum time required to attain pasteurization in September is at noon and it is 4.2 min and 6 min for FPSC integrated with and without reflector, respectively. Furthermore, in November, the minimum time required to attain pasteurization is at noon and is 3.9 min and 5.72 min for FPSC integrated with and without reflector.

(ii) The daily pasteurized milk production in September is 58.59 l/day and 69.19 l/day for FPSC integrated with and without reflector, respectively. Also, the daily pasteurized milk production in November is 60.2 l/day and 70.2 l/day for FPSC integrated with and without reflector, respectively. Due to the integration of the reflector, an increment of pasteurized milk production of 9 l/day is achieved.

(iii) The system successfully attains pasteurization temperature along with acceptable milk quality

(which is tested using the methylene blue reduction test method)

(iv) This device avails the use of solar energy for milk pasteurization has great potential for the rural populations that rely on milk as a primary source of income by extending the shelf life of milk.

Nomenclature

A_c: Area of the collector
D_i: Tube inner diameter
E_{x_d}: Destructed exergy
$E_{d_{p-s}}$: Exergy distraction caused by the temperature difference between the absorber plate and solar radiation
$E_{d_{p-f}}$: Exergy distraction caused by the temperature difference between the absorber plate surface and working fluid
$E_{x_{\text{in}}}$: Inlet exergy
$E_{x_{\text{inf}}}$: Inlet exergy rate due to the fluid flow
$E_{x_{\text{inr}}}$: Inlet exergy due to radiation
E_{x_l}: Leakage exergy
$E_{x_{\text{out}}}$: Outlet exergy
F_R: Collector heat removal factor
$\dot{m}$: Mass flow rate
Q_{ab}: Absorbed energy
q_{day}: Quantity of pasteurized milk per day
Q_l: Thermal loss
Q_u: Useful energy gain
T_a: Ambient temperature
T_g: Glass temperature
T_p: Absorber plate temperature
T_o: Outlet temperature
T_{pm}: Mean plate temperature.

Data Availability

The data used to support the findings of this study are available from the corresponding author upon request.

Disclosure

This manuscript is a part of an academic thesis presented to the University of Gondar, Gondar, Ethiopia.

Conflicts of Interest

The authors declare that they have no conflicts of interest.

Acknowledgments

The authors sincerely thank the staff members of the University of Gondar, Department of Mechanical Engineering and Chemistry, for their support during experimentation and milk quality checking.

References

[1] USAID, *The Future of Livestock in Nigeria: Opportunities and Challenges in the Face of Uncertainty*, Food and Agriculture Organization of the United Nations, Italy, Rome, 2019.

[2] "Study on dairy investment opportunities in Ethiopia," 2008, https://www.bibalex.org/search4dev/files/337939/171402.pdf.

[3] T. Alemneh, T. Alemneh, and D. Akeberegn, "Dairy production in Ethiopia-existing scenario and constraints," *Biomedical Journal of Scientific & Technical Research*, vol. 16, no. 5, pp. 12304–12309, 2019.

[4] M. A. M. Ahmed, S. Ehui, and A. Yemesrach, "Dairy development in Ethiopia EPTD discussion paper no. 123 dairy development in Ethiopia," 2004, https://www.ifpri.org/publication/dairy-development-ethiopia.

[5] H. W. Woldemariam and A. M. Asres, "Microbial and physicochemical qualities of pasteurized milk," *Journal of Food Processing & Technology*, vol. 8, no. 1, 2017.

[6] "Heat treatment of milk-overview," 2018, https://fil-idf.org/wp-content/uploads/2018/02/Factsheet-001_Heat-treatment-1-1.pdf.

[7] A. Dingeto Hailu and D. Kalbessa Kumsa, "Ethiopia renewable energy potentials and current state," *AIMS Energy*, vol. 9, no. 1, pp. 1–14, 2021.

[8] S. A. Mekonnen, "Solar energy assessment in Ethiopia: modeling and measurement," 2007, http://213.55.95.56/bitstream/handle/123456789/6866/Sharew%20Anteneh.pdf?sequence=1&isAllowed=y.

[9] A. K. Chaturvedi, "A review of solar flat plate liquid collector's components," *International Journal of Advance Research and Innovation*, vol. 3, no. 1, pp. 138–141, 2015.

[10] T. Mihret, F. Mitku, and T. Guadu, "Dairy farming and its economic importance in Ethiopia: a review," *World Journal of Dairy & Food Sciences*, vol. 12, no. 1, pp. 42–51, 2017.

[11] R. Ruben, A. Dekeba Bekele, and B. Megersa Lenjiso, "Quality upgrading in Ethiopian dairy value chains: dovetailing upstream and downstream perspectives," *Review of Social Economy*, vol. 75, no. 3, pp. 296–317, 2017.

[12] S. Watts, "A mini review on technique of milk pasteurization," *Journal of Pharmacognosy and Phytochemistry*, vol. 5, no. 5, pp. 99–101, 2016.

[13] K. M. Nielsen and T. S. Pedersen, "Solar panel based milk pasteurization," 2001, https://vbn.aau.dk/ws/portalfiles/portal/169406/fulltext.

[14] F. O. Wayua, M. W. Okoth, and J. Wangoh, "Design and performance assessment of a flat-plate solar milk pasteurizer for arid pastoral areas of Kenya," *Journal of Food Processing and Preservation*, vol. 37, no. 2, pp. 120–125, 2013.

[15] M. F. M. Atia, M. Mostafa, M. El-Nono, and M. Abdel-Salam, "Solar energy utilization for milk pasteurization," *Misr Journal of Agricultural Engineering*, vol. 28, pp. 729–744, 2011.

[16] J. Franco, L. Saravia, V. Javi, R. Caso, and C. Fernandez, "Pasteurization of goat milk using a low cost solar concentrator," *Solar Energy*, vol. 82, no. 11, pp. 1088–1094, 2008.

[17] M. F. M. Atia, M. M. Mostafa, M. A. El-Nono, and M. F. Abdel-Salam, "Milk pasteurization using solar concentrator with tracking device," *Misr Journal of Agricultural Engineering*, vol. 33, no. 3, pp. 915–932, 2016.

[18] D. Degefa, "Performance analysis of small-scale milk pasteurization using solar thermal energy," 2018, http://213.55.95.56/bitstream/handle/123456789/18369/Derese%20Degefa.pdf?sequence=1&isAllowed=y.

[19] J. Mallett, "Concentrated solar power development for milk pasteurization in rural South Africa," 2019, https://scholar.sun.ac.za/handle/10019.1/105777.

[20] Z. Said, P. Sharma, A. K. Tiwari et al., "Application of novel framework based on ensemble boosted regression trees and Gaussian process regression in modelling thermal performance of small-scale organic rankine cycle (ORC) using hybrid nanofluid," *Journal of Cleaner Production*, vol. 360, Article ID 132194, 2022.

[21] M. Chegaar, A. Lamri, and A. Chibani, "Estimating global solar radiation using sunshine hours," *Revue des Energies Renouvelables: Physique Energétique*, vol. 1998, p. 11, 1998.

[22] J. A. Prescott, "Evaporation from water surface in relation to solar radiation," *Transactions of the Royal Society of South Australia*, vol. 64, pp. 114–118, 1940.

[23] M. A. Akgün, "Heat removal factor for a serpentine absorberplate," *Solar Energy*, vol. 41, no. 1, pp. 109–111, 1988.

[24] H. R. Thornton and R. B. Sandin, "Standardization of the methylene blue reduction test by the use of methylene blue thiocyanate," *American Journal of Public Health and the Nation's Health*, vol. 25, no. 10, pp. 1114–1117, 1935.

[25] S. K. Nandy and K. V. Venkatesh, "Application of methylene blue dye reduction test (MBRT) to determine growth and death rates of microorganisms," *African Journal of Microbiology Research*, vol. 4, no. 1, pp. 61–70, 2010.

[26] S. S. Anwer, S. M. Zaki, S. A. Rasul, R. J. Hassan, I. J. Ahmad, and A. J. Qader, "Detection of kids milk quality using methylene blue reduction test," *International Journal of Environment, Agriculture and Biotechnology*, vol. 3, no. 4, pp. 1450–1456, 2018.

[27] S. N. Chatterjee, I. Bhattacharjee, S. K. Chatterjee, and G. Chandra, "Microbiological examination of milk in Tarakeswar, India with special reference to coliforms," *African Journal of Biotechnology*, vol. 5, no. 15, pp. 1383–1385, 2006.

[28] M. Pérez-Lomas, M. J. Cuaran-Guerrero, L. Yépez-Vásquez et al., "The extended methylene blue reduction test and milk quality," *Foods and Raw Materials*, vol. 8, no. 1, pp. 140–148, 2020.